

Transverse Asymmetry of the Index Modulation Profile in Few-Mode Fiber Bragg Grating

Peihong Guan, Min Tang, Min Cao, Yuean Mi, Mei Liu, Wenhua Ren and Guobin Ren * 

Key Laboratory of All Optical Network and Advanced Telecommunication Network, Ministry of Education, Institute of Lightwave Technology, Beijing Jiaotong University, Beijing 100044, China; 18120004@bjtu.edu.cn (P.G.); 16111010@bjtu.edu.cn (M.T.); 15111023@bjtu.edu.cn (M.C.); 14111041@bjtu.edu.cn (Y.M.); 18120009@bjtu.edu.cn (M.L.); whren@bjtu.edu.cn (W.R.)

* Correspondence: gbren@bjtu.edu.cn

Abstract: The transverse asymmetry of the index modulation profile in the asymmetric few-mode fiber Bragg grating (FM-FBG) was investigated. The transverse asymmetry of the index modulation profile will lead to mode conversion between modes with the different azimuthal orders, and this asymmetry is characterized by the attenuation coefficient α . We evaluated that the value of attenuation coefficient α was $0.2 \mu\text{m}^{-1}$, and grating amplitude χ was 2.8×10^{-4} for FM-FBG inscribed by UV single-side illumination. We found that the optimized value of α was $0.16 \mu\text{m}^{-1}$, at which the maximum mode conversion efficiency of LP_{01} – LP_{11} can be achieved. The results of this paper provide great potential application in few-mode fiber (FMF) devices and mode division multiplexing (MDM) optical communication.

Keywords: fiber Bragg grating; few-mode fiber; mode conversion; transverse asymmetry



Citation: Guan, P.; Tang, M.; Cao, M.; Mi, Y.; Liu, M.; Ren, W.; Ren, G. Transverse Asymmetry of the Index Modulation Profile in Few-Mode Fiber Bragg Grating. *Photonics* **2021**, *8*, 87. <https://doi.org/10.3390/photonics8030087>

Received: 16 January 2021

Accepted: 19 March 2021

Published: 23 March 2021

Publisher's Note: MDPI stays neutral with regard to jurisdictional claims in published maps and institutional affiliations.



Copyright: © 2021 by the authors. Licensee MDPI, Basel, Switzerland. This article is an open access article distributed under the terms and conditions of the Creative Commons Attribution (CC BY) license (<https://creativecommons.org/licenses/by/4.0/>).

1. Introduction

In recent years, few-mode fiber Bragg grating (FM-FBG) has attracted considerable attention, owing to the advantages of simple structure, flexible operation, versatility, low loss, and low crosstalk [1]. The FM-FBGs can realize the coupling of the forward propagating mode and the phase-matched backward propagating mode, which are widely used in various applications such as fiber filters [2], fiber lasers [3–5], fiber sensors [6,7], mode division multiplexing (MDM) communication systems [8], and mode converters (MCs) [9–12].

As one of the key components in an MDM system, the MCs based on FM-FBG can convert a specific mode into other modes. Traditionally, for a uniform FM-FBG, the mode conversion only occurs between modes with the same azimuthal order. However, when FM-FBG has an asymmetric transverse index profile, the mode can convert into the higher azimuthal order modes [13,14]. A high-order vector mode conversion approach was proposed based on asymmetric fiber Bragg grating (AFBG), and the influence of the attenuation coefficient α on vector mode conversion was also theoretically analyzed, and the maximum conversion efficiency at specific α was achieved for each vector mode [15]. Additionally, some experiments on asymmetric FM-FBG were also reported. The strong LP_{01} and LP_{11} mode coupling was experimentally achieved by Wu et al. [16] through ultra-violet (UV) illumination on the fiber from one side. Wang et al. [17] realized the mode conversion of high-order vector mode (including TE_{01} , TM_{01} , HE_{21} , HE_{31} , and EH_{11}) based on AFBG. Moreover, Yao et al. [18] designed experiments to realize high-order excitation modes by a lateral core offset splicing spot (OSS), and mode conversion from LP_{01} to LP_{01} , LP_{01} to LP_{11} , LP_{11} to LP_{11} , LP_{11} to LP_{21} , and LP_{11} to LP_{21} was demonstrated through UV single-side illumination. With the single-side illumination of UV light, the refractive index modulation profile across the fiber core in FM-FBG could change asymmetrically [19]. The transverse asymmetry is characterized by the attenuation coefficient α . Therefore, the determination

of the attenuation coefficient α of FM-FBG is significant for realizing high-order mode conversion. The value of α was generally obtained by a fit of transverse index profile across the core according to measured transverse index data in the experiment [20,21]. However, the scheme mentioned above is relatively complicated.

In this paper, we propose a method to determine the value of α according to the transmission spectrum of FM-FBG combined with coupled mode theory. The values of α and χ were obtained for the FBGs inscribed in the homemade few-mode fiber (FMF) by UV single-side illumination. Based on the obtained α and χ , we calculated the transmission spectra of FM-FBG, which is consistent with the experimental results of FM-FBG. Furthermore, the optimization of α was analyzed under different excitations (LP₀₁ mode, LP₁₁ mode).

2. Simulation and Experiment

We studied the mode conversion based on asymmetric FBG in a homemade FMF. The homemade FMF was fabricated via modified chemical vapor deposition (MCVD), and its refractive index profile is shown in Figure 1a. The fiber core diameter was approximately 15 μm , and the max core-cladding index difference was 0.008. The first three linearly polarized modes (LP₀₁, LP₁₁, and LP₂₁ modes) were supported at C band for this FMF. The effective refractive indices of LP₀₁ mode, LP₁₁ mode, and LP₂₁ mode were 1.4495, 1.4477, and 1.4451 at the wavelength of 1550 nm, respectively. Based on the coupled mode theory, strong mode coupling would occur when the phase matching condition was satisfied [22], expressed as $\Delta n = \beta_m + \beta_n - 2K$, where β_m and β_n are propagation constants of the m th forward mode and n th backward mode. K is the wave number of non-tilted grating, and $K = \pi/\Lambda$, where Λ is the period of grating, and a phase mask with period of 1068 nm is used to inscribe FM-FBG. The variation of Δn^+ with wavelength is shown in Figure 1b. Among them, the solid lines and the dashed lines indicate that the excitation was LP₀₁ mode and LP₁₁ mode, respectively. And the red lines, black lines, and blue lines represent coupled LP₀₁ mode, LP₁₁ mode, and LP₂₁ mode, respectively. The wavelength corresponding to $\Delta n^+ = 0$ was the resonance wavelength of the coupled modes. For example, when the excitation was LP₀₁ mode, the resonance wavelength of the coupled LP₁₁ mode was 1546.5 nm. The values of resonance wavelength of each coupled mode under different excitation modes are listed in Table 1. Here, LP₀₁-LP₀₁ (LP₁₁-LP₁₁) represents the self-coupling (intra-mode coupling) process, and LP₀₁-LP₁₁ (LP₀₁-LP₂₁, LP₁₁-LP₀₁, LP₁₁-LP₂₁) represents the cross-coupling (inter-mode coupling) process.

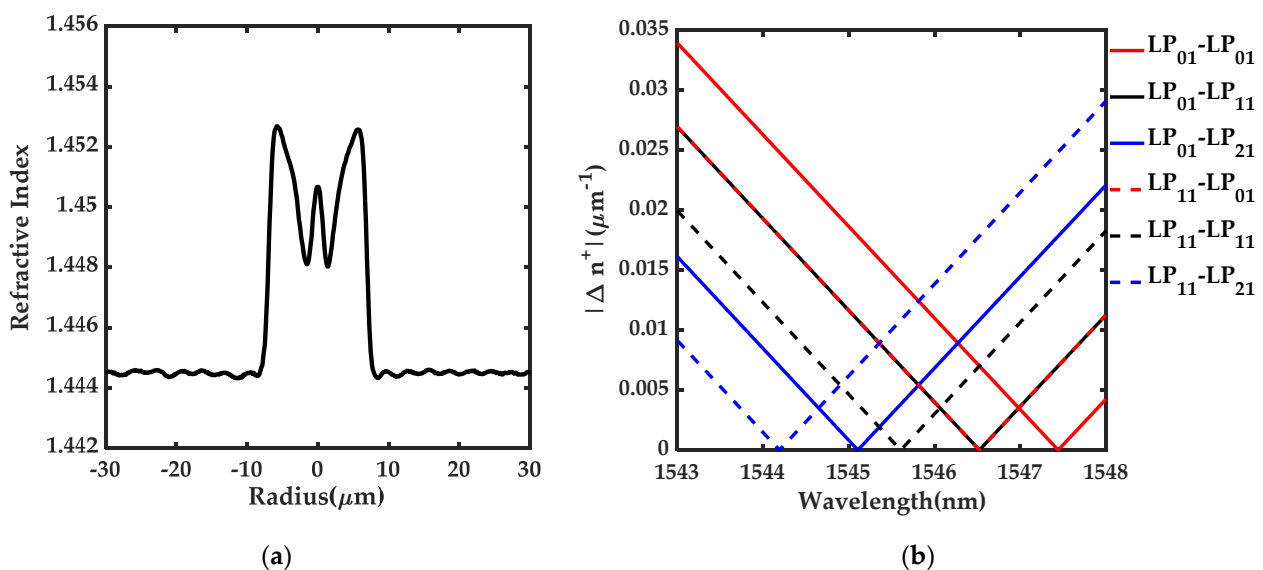


Figure 1. (a) The refractive index profile of the homemade few-mode fiber (FMF). (b) Phase matching expression Δn^+ as a function of wavelength.

Table 1. The resonance wavelengths of coupled modes under different excitation modes.

Excitation Modes–Coupled Modes	Resonance Wavelengths (nm)
LP ₀₁ –LP ₀₁	1547.4
LP ₀₁ –LP ₁₁	1546.5
LP ₀₁ –LP ₂₁	1545.1
LP ₁₁ –LP ₀₁	1546.5
LP ₁₁ –LP ₁₁	1545.6
LP ₁₁ –LP ₂₁	1544.2

When FM-FBG was fabricated by UV single-side illumination, and the fiber core on the side close to the UV beam had the higher refractive index change because of the absorption of UV light. Therefore, the refractive index profile over the fiber core became asymmetric after UV single-side illumination [19]. The refractive index modulation is an approximate decreasing exponential profile (as shown in Figure 2), and the core refractive index modulation function could be expressed as [15]:

$$\Delta n(z) = \sigma(z) + 2\chi \cdot \exp[-\alpha(x + \sqrt{r_{co}^2 - y^2})] \cdot \cos[\frac{2\pi}{\Lambda}z + \phi(z)] \tag{1}$$

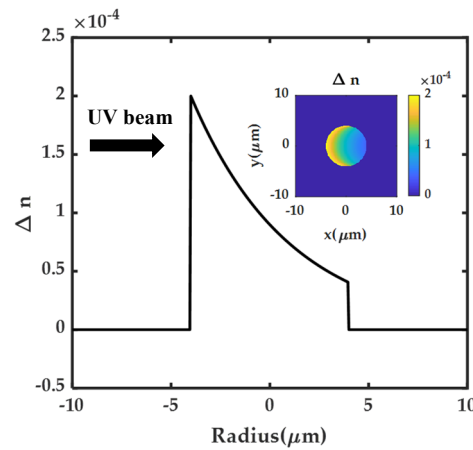


Figure 2. Asymmetric refractive index modulation by UV single-side illumination.

The coupling coefficient κ_{mn} of the m th and n th modes can be represented as [15,16]:

$$\kappa_{mn} = \frac{\epsilon_0 \omega}{2} \iint n(r)P(r)(E_m \cdot E_n)\Delta n(z)dS \tag{2}$$

where $\sigma(z)$ is the slow varying DC perturbation. Here, $\sigma(z) = 0$. χ is the grating amplitude, and α is the attenuation coefficient of the index change distribution. $\phi(z)$ is the chirp function of the grating. r_{co} is the radius of the fiber core, and Λ is the grating period. ϵ_0 is the dielectric constant. ω is the angular frequency of light. $n(r)$ is the refractive index of the fiber. $P(r)$ is the function on the fiber radius, r ($P(r) = 1$, inside the perturbed area; $P(r) = 0$, outside the perturbed area). Finally, E_m and E_n are the normalized electric fields of the m th and n th modes, respectively. Therefore, α and χ will affect the mode coupling efficiency by Equation (2).

Figure 3a,b show the transmission spectra of the FM-FBG when the excitation (input mode) is LP₀₁ mode and LP₁₁ mode, respectively. The black lines, red lines, and blue lines represent the transmission spectra of the coupled LP₀₁ mode, LP₁₁ mode, and LP₂₁ mode, respectively. Here, we adopt $\alpha = 0.2 \mu\text{m}^{-1}$, $\chi = 2 \times 10^{-4}$, and a grating length $L = 13 \text{ mm}$. In Figure 3a, LP₀₁ mode was used as the excitation mode, and the transmission peak of LP₀₁ mode (LP₁₁ mode) was -20.1 dB (-8.9 dB) at a wavelength of $1.5474 \mu\text{m}$ ($1.5465 \mu\text{m}$), which corresponds to conversion efficiency of 99% (87%). However, the transmission of LP₂₁ mode was very small and can be ignored (as shown in the set in Figure 3a). LP₁₁ mode was used as the excitation mode, and the transmission spectrum of the FM-FBG is shown in

Figure 3b. The transmission peaks of LP₀₁ mode, LP₁₁ mode, and LP₂₁ mode were −8.9 dB, −21.6 dB, and −5.1 dB at the wavelengths of 1.5465 μm, 1.5456 μm, and 1.5442 μm, which correspond to conversion efficiencies of 87%, 99.3%, and 69%, respectively. The resonance wavelength corresponding to each coupled mode was consistent with the results in Table 1. Moreover, compared with the mode conversion from LP₀₁ mode to LP₂₁ mode, the mode conversion from LP₁₁ mode to LP₂₁ mode was stronger because of the large overlap of the mode fields. Therefore, when the excitation was in LP₁₁ mode, strong LP₁₁ and LP₂₁ mode conversion could be realized. Meanwhile, no matter which mode is used as the excitation, the self-coupling process was stronger than the cross-coupling process.

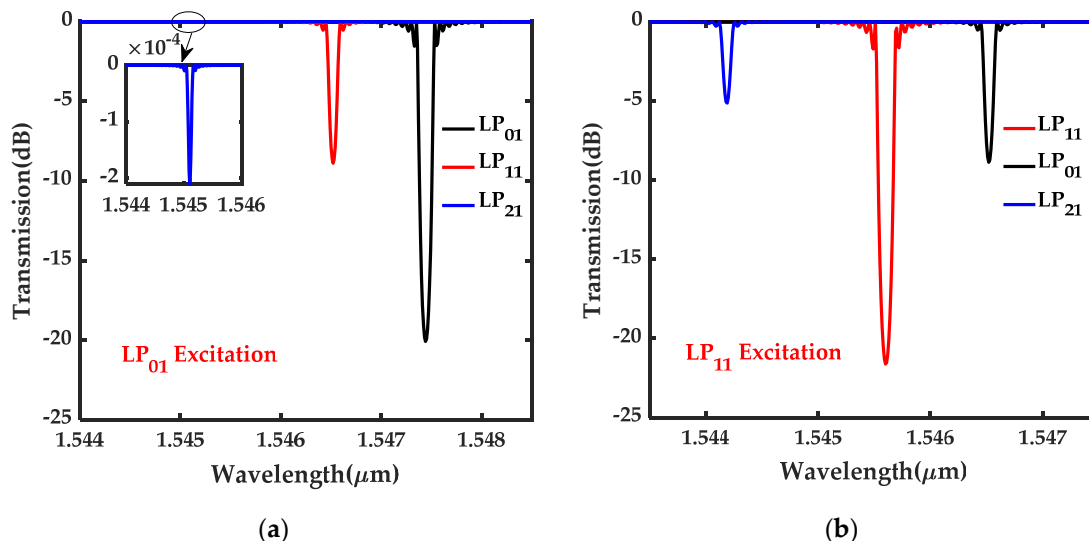


Figure 3. Transmission spectra of the few-mode fiber Bragg grating (FM-FBG) when the excitation was (a) LP₀₁ mode and (b) LP₁₁ mode.

According to the index modulation expression of asymmetric FM-FBG (Equation (1)), the attenuation coefficient α and the grating amplitude χ affected the refractive index profile of fiber core and further affected the mode coupling coefficient by Equation (2), and finally determined the output characteristics of the FM-FBG. α was determined by the absorption factor of the material, and χ depended on the UV power and the photosensitivity of the fiber [16]. When the excitation was in LP₀₁ mode, the variations in the conversion efficiencies of the LP₀₁ mode and LP₁₁ mode with α and χ are shown in Figure 4a,b. At a given α , the conversion efficiencies of the coupled LP₀₁ mode and LP₁₁ mode increased with the increase in χ . Moreover, with a given χ , as α increased, the mode conversion efficiency of self-coupling (LP₀₁–LP₀₁) decreased, and the mode conversion efficiency of cross-coupling (LP₀₁–LP₁₁) increased firstly from zero to the maximum and then decreased. Therefore, with a given χ , the maximum mode conversion efficiency from the LP₀₁ mode to the LP₁₁ mode can be achieved at a specific α .

Next, in the experiment, we investigated mode conversion based on asymmetric FM-FBG1, and the FM-FBG1 was written in the homemade FMF by the well-established phase mask method under UV single-side illumination [16,23]. The experimental setup included amplified spontaneous emission (ASE) light source, single-mode fiber (SMF), few-mode fiber (FMF), and an optical spectrum analyzer (OSA). The ASE light source enters from SMF to FMF, and then the transmitted light from FMF is output through SMF and the transmission spectrum is monitored by OSA. During splicing of SMF and FMF, the axes of SMF and FMF are aligned without introducing lateral core OSS. Since the homemade FMF supports LP₀₁, LP₁₁, and LP₂₁ modes and does not support LP₀₂ mode (LP₀₂ mode is cutoff), it can be determined that the excitation mode in the experiment was LP₀₁ mode and no other modes were excited [16]. The length of FM-FBG1 was 13 mm. The values of laser energy, voltage, frequency, and moving speed of the displacement platform were 60 mJ, 19.15 kv, 20 Hz, and 0.2 mm/s, respectively. The experimental results of the

transmission spectra of FM-FBG1 are shown as the blue lines in Figure 5a. The two peaks (i) and (ii) corresponding to self-coupling (LP_{01} – LP_{01}) and cross-coupling (LP_{01} – LP_{11}) are centered at the wavelengths of 1547.3 nm and 1546.3 nm, respectively. In addition, the values of the transmission peaks (i) and (ii) were -27.8 dB and -13.9 dB, which correspond to conversion efficiencies of 99.83% and 95.93%, respectively. The two red lines in Figure 4a,b show the contour lines of 0.9983 and 0.9593, respectively. According to the intersection point of the two red lines, we obtained $\alpha \approx 0.2 \mu\text{m}^{-1}$ and $\chi \approx 2.8 \times 10^{-4}$.

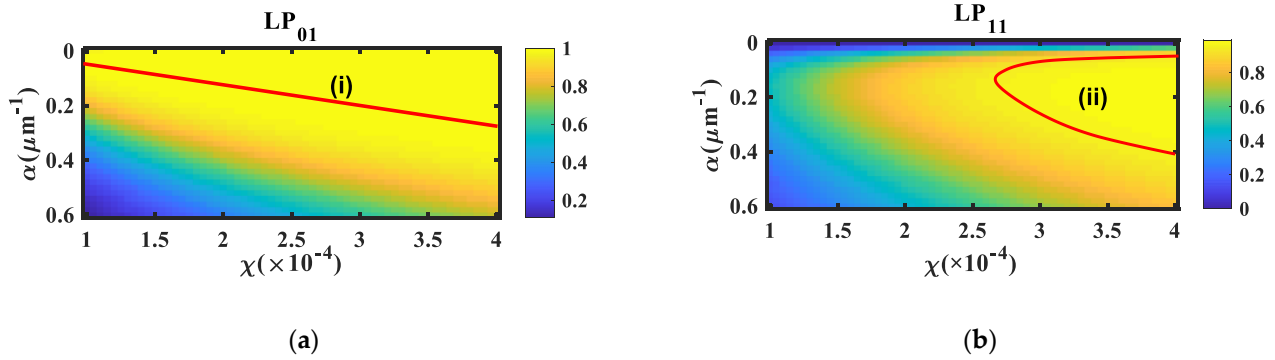


Figure 4. The conversion efficiencies of the (a) LP_{01} mode and (b) LP_{11} mode versus attenuation coefficient α and grating amplitude χ under LP_{01} mode excitation (red lines (i) and (ii) are contour lines of 0.9983 and 0.9593, respectively).

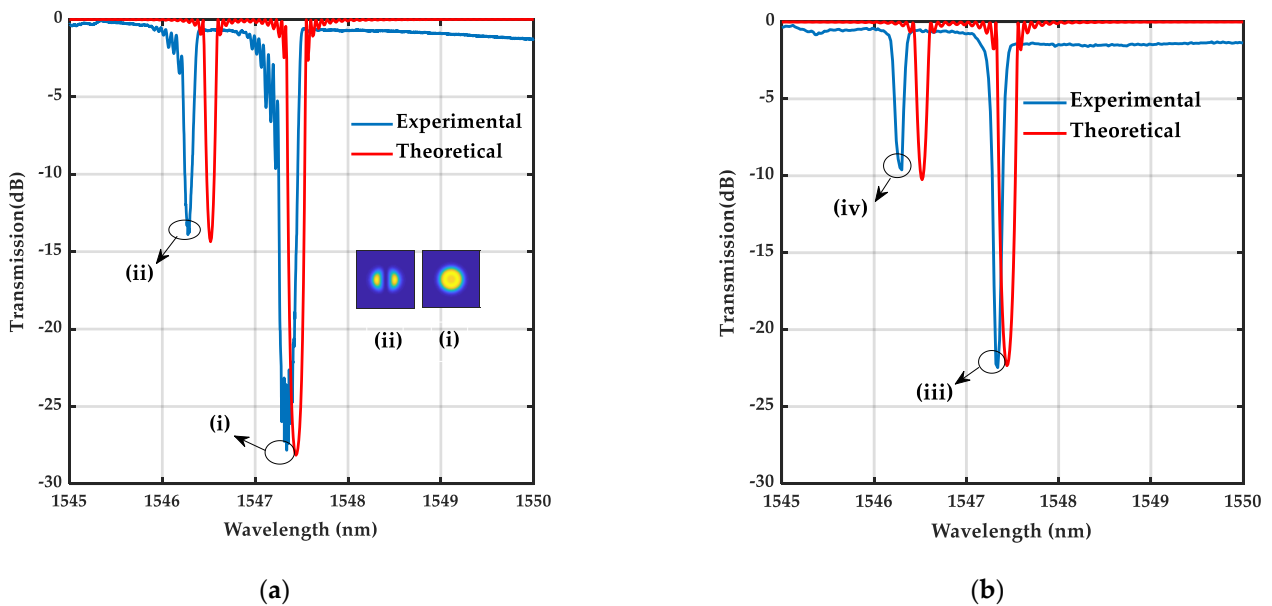


Figure 5. Theoretical and experimental results of the transmission spectra of (a) FM-FBG1 and (b) FM-FBG2 under LP_{01} mode excitation.

Then based on the obtained α and χ , the theoretical result of transmission spectra is shown as the red lines in Figure 5a. The values of transmission peak (conversion efficiency) of LP_{01} – LP_{01} and LP_{01} – LP_{11} were -28.1 dB (99.85%) and -14.3 dB (96.28%), respectively. And the resonance wavelengths of these two peaks were 1547.4 nm and 1546.5 nm, respectively. Therefore, the values of the theoretical transmission peak were consistent with the experimental results. Note that the resonance wavelengths of the simulation showed a slight difference from the experimental result, and we believe this difference was caused by the external tension in the processing of fabricating FM-FBG. The external tension would cause the strain change of grating, and the resonance Bragg wavelength shift varied linearly with the strain change [24,25]. Since our experiments were operated at room temperature, the effect of temperature was not considered. The Bragg wavelength shift, $\Delta\lambda_B$, can be expressed as $\Delta\lambda_B = \lambda_B(1 - P_e)\Delta\varepsilon_{FBG}$, where P_e is the photo-

elastic constant (0.22), and $\Delta\varepsilon_{FBG}$ is the strain change of FM-FBG. λ_B is the initial resonance Bragg wavelength. Thus, strain sensitivities were approximately 1.207 pm/microstrain and 1.206 pm/microstrain, $\Delta\lambda_{01} = 1.207\Delta\varepsilon_{FBG}$ and $\Delta\lambda_{11} = 1.206\Delta\varepsilon_{FBG}$, $\Delta\lambda_{01}$ and $\Delta\lambda_{11}$ represent the Bragg wavelength shift of the coupled LP₀₁ and LP₁₁ modes under LP₀₁ mode excitation. Therefore, under the external tension, the resonance wavelength will shift linearly. Theoretically $\Delta\lambda_{01}$ and $\Delta\lambda_{11}$ should be approximately consistent. However, comparing the experimental and simulation results, $\Delta\lambda_{01} = 0.1$ nm and $\Delta\lambda_{11} = 0.2$ nm, the resonance Bragg wavelength shift of LP₁₁ was larger than that of LP₀₁. This may be due to the non-uniformity of the refractive index profile along the length of the homemade fiber. This non-uniformity will affect the effective refractive indices of LP₀₁ and LP₁₁ modes, and result in error of the resonance wavelength shift.

Also, in the experiment, the FM-FBG2 was written in the homemade FMF through UV single-side illumination under LP₀₁ mode excitation, and the grating length was 10 mm. The experimental result of the transmission spectra of FM-FBG2 is shown as the blue lines in Figure 5b. The two peaks (iii) and (iv) were centered at the wavelengths of 1547.34 nm and 1546.3 nm, respectively, and the values of the transmission peaks (iii) and (iv) were -22.47 dB and -9.62 dB, which correspond to conversion efficiencies of 99.43% and 89.09%, respectively. Since the parameters of the two experiments are the same except for the grating length, α and χ were the same. Based on the obtained α and χ , we calculated the transmission spectra of FM-FBG2 (as shown by the red lines in Figure 5b). The values of the transmission peak (conversion efficiency) of LP₀₁-LP₀₁ and LP₀₁-LP₁₁ were -22.3 dB (99.41%) and -10.2 dB (90.45%), which are consistent with the experimental results of FM-FBG2. Moreover, the shift of the resonance wavelength of FM-FBG2 was also due to the external tension, which is in accordance with the reason for the FM-FBG1. In addition, comparing the transmission spectra of FM-FBG1 and FM-FBG2, the mode conversion efficiencies increased as the grating length increases.

The mode conversion characteristics of FM-FBG1 could be further improved by optimizing α . Figure 6a,b show the variations of the mode conversion efficiencies with the attenuation coefficient α , when excitation was LP₀₁ mode and LP₁₁ mode, respectively. The black lines, red lines, and blue lines represent coupled LP₀₁ mode, LP₁₁ mode, and LP₂₁ mode, respectively. When $\alpha = 0$, only self-coupling (LP₀₁-LP₀₁, LP₁₁-LP₁₁) occurs. With the increase of α , the mode conversion efficiencies of self-coupling gradually decreased. The mode conversion efficiencies of cross-coupling (LP₀₁-LP₁₁, LP₁₁-LP₀₁, LP₁₁-LP₂₁) increased firstly and then decreased with the increase of α and reached the maximum when $\alpha = 0.16 \mu\text{m}^{-1}$. It should be noted that the FM-FBG inscribed by the phase mask method have the advantages of low cost, simple structure and easy to fabricate. Moreover, the FM-FBG can be applied to MDM optical communication, optical fiber lasers and optical fiber sensors, due to the fact of its mode conversion functions.

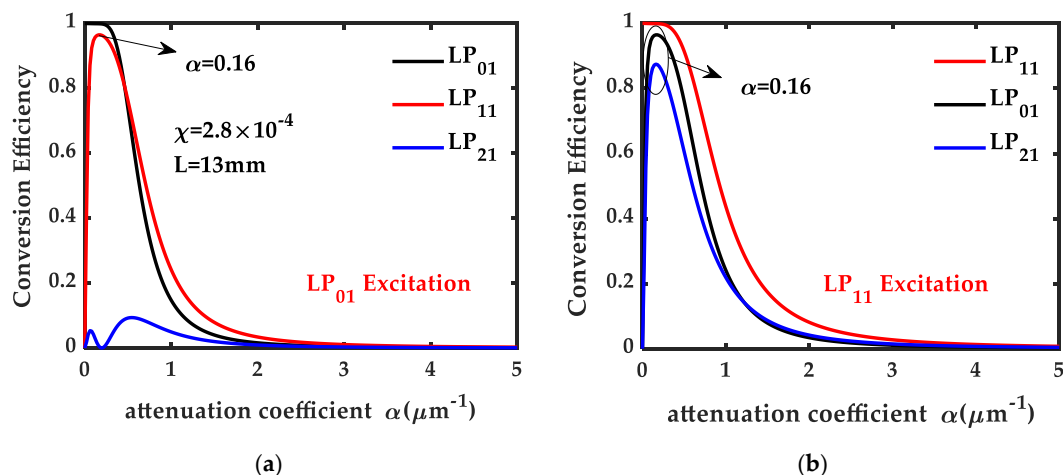


Figure 6. The conversion efficiencies versus attenuation coefficient α when excitation was (a) LP₀₁ mode and (b) LP₁₁ mode.

3. Conclusions

In conclusion, we investigated the transverse asymmetry of the index modulation profile in the asymmetric FBG written in a homemade FMF by UV single-side illumination, and the asymmetry can be represented by the attenuation coefficient α . When LP₀₁ mode was used as the excitation mode, the values of α and grating amplitude χ were evaluated, and α was approximately $0.2 \mu\text{m}^{-1}$ and χ at a speed of 0.2 mm/s in the experiment was approximately 2.8×10^{-4} . Based on the obtained α and χ , we calculated the transmission spectra of FM-FBG. The theoretical results of the transmission spectra were in accordance with the experimental results, which show that the obtained α and χ were feasible. In addition, the maximum mode conversion efficiencies of cross-coupling were achieved by the optimized value of α ($0.16 \mu\text{m}^{-1}$). This work can be applied to the fields of FMF devices and MDM optical communication.

Author Contributions: Conceptualization, P.G. and G.R.; Data curation, P.G.; Funding acquisition, W.R.; Investigation, P.G.; Methodology, P.G. and G.R.; Software, P.G.; Supervision, G.R.; Writing—original draft, P.G.; Writing—review & editing, P.G., M.T., M.C., Y.M., M.L., W.R. and G.R. All authors have read and agreed to the published version of the manuscript.

Funding: National Natural Science Foundation of China (NSFC) (62075008).

Conflicts of Interest: The authors declare no conflict of interest.

References

1. Erdogan, T. Fiber grating spectra. *J. Lightwave Technol.* **1997**, *15*, 1277–1294. [[CrossRef](#)]
2. Jiang, J.; Qiu, H.; Wang, G.; Li, Y.; Dai, T.; Wang, X.; Yu, H.; Yang, J.; Jiang, X. Broadband tunable filter based on the loop of multimode Bragg grating. *Opt. Express* **2018**, *26*, 559–566. [[CrossRef](#)]
3. Liu, T.; Chen, S.; Hou, J. Selective transverse mode operation of an all-fiber laser with a mode-selective fiber Bragg grating pair. *Opt. Lett.* **2016**, *41*, 5692–5695. [[CrossRef](#)]
4. Jin, W.; Qi, Y.; Yang, Y.; Jiang, Y.; Wu, Y.; Xu, Y.; Yao, S.; Jian, S. Switchable dual-mode all-fiber laser with few-mode fiber Bragg grating. *J. Opt.* **2017**, *19*, 095702. [[CrossRef](#)]
5. Li, H.; Yan, K.; Dong, Z.; Tao, R.; Gu, C.; Yao, P.; Xu, L.; Zhang, R.; Su, J.; Zhan, Q. Multi-wavelength oscillating and transverse mode switching in an all few-mode fiber laser based on polarization manipulation. *Opt. Laser Technol.* **2019**, *117*, 110–113. [[CrossRef](#)]
6. Albert, J.; Shao, L.; Caucheteur, C. Tilted fiber Bragg grating sensors. *Laser Photonics Rev.* **2013**, *7*, 83–108. [[CrossRef](#)]
7. Liu, A.; Fan, W.; Fan, L. A High Sensitive Borehole Strainmeter based on Fiber Bragg Grating. In Proceedings of the 2018 Asia Communications and Photonics Conference (ACP), New Century Grand Hotel, Hangzhou, China, 26–29 October 2018; Optical Society of America: Hangzhou, China, 2018.
8. Gao, Y.; Sun, J.; Chen, G.; Sima, C. Demonstration of simultaneous mode conversion and demultiplexing for mode and wavelength division multiplexing systems based on tilted few-mode fiber Bragg gratings. *Opt. Express* **2015**, *23*, 9959–9967. [[CrossRef](#)] [[PubMed](#)]
9. Xiao, R.; Shi, Y.; Li, J.; Dai, P.; Zhao, Y.; Li, L.; Lu, J.; Chen, X. On-chip mode converter based on two cascaded Bragg gratings. *Opt. Express* **2019**, *27*, 1941–1957. [[CrossRef](#)]
10. Zhang, X.; Wang, A.; Chen, R.; Zhou, Y.; Ming, H.; Zhan, Q. Generation and Conversion of Higher Order Optical Vortices in Optical Fiber With Helical Fiber Bragg Gratings. *J. Lightwave Technol.* **2016**, *34*, 2413–2418. [[CrossRef](#)]
11. Ali, M.M.; Jung, Y.; Lim, K.S.; Islam, M.R.; Alam, S.U.; Richardson, D.J.; Ahmad, H. Characterization of Mode Coupling in Few-Mode FBG With Selective Mode Excitation. *IEEE Photonic Tech. Lett.* **2015**, *27*, 1713–1716. [[CrossRef](#)]
12. Yang, K.; Liu, Y.G.; Wang, Z.; Li, Y.; Mao, B.W. Triple-order Orbital-angular-momentum modes generation based on single tilted fiber Bragg grating in a few-mode ring-core fiber. *Opt. Fiber Technol.* **2020**, *55*, 102155. [[CrossRef](#)]
13. Thomas, J.; Jovanovic, N.; Becker, R.G.; Marshall, G.D.; Withford, M.J.; Tünnermann, A.; Nolte, S.; Steel, M.J. Cladding mode coupling in highly localized fiber Bragg gratings: Modal properties and transmission spectra. *Opt. Express* **2011**, *19*, 325–341. [[CrossRef](#)]
14. Yang, R.; Xue, Y.; Chen, C.; Wang, C.; Guo, J.C. Mode Coupling Characteristics for Fiber Bragg Gratings with Asymmetric Refractive Index Profile. In Proceedings of the 1st International Conference on Frontiers of Laser Processing (ICFL), Chang chun, China, 11–15 July 2011.
15. Mi, Y.; Li, H.; Ren, G. Vector mode conversion based on an asymmetric fiber Bragg grating in few-mode fibers. *Appl. Opt.* **2017**, *56*, 7305–7310. [[CrossRef](#)]
16. Wu, C.; Liu, Z.; Chung, K.M.; Tse, M.L.V.; Tam, H.Y. Strong LP 01 and LP 11 mutual coupling conversion in a two-mode fiber Bragg grating. *IEEE Photonics J.* **2012**, *4*, 1080–1086. [[CrossRef](#)]

17. Wang, L.; Vaity, P.; Ung, B.; Messaddeq, Y.; Rusch, L.A.; Larochele, S. Characterization of OAM fibers using fiber Bragg gratings. *Opt. Express* **2014**, *22*, 15653–15661. [[CrossRef](#)]
18. Yao, S.Z.; Ren, G.; Yang, Y.; Shen, Y.; Jiang, Y. Few-mode fiber Bragg grating-based multi-wavelength fiber laser with tunable orbital angular momentum beam output. *Laser Phys. Lett.* **2018**, *15*, 095001. [[CrossRef](#)]
19. Renner, H. Effective-index increase, form birefringence and transition losses in UV-side-illuminated photosensitive fibers. *Opt. Express* **2001**, *9*, 546–560. [[CrossRef](#)]
20. Dossou, K.; Larochele, S.; Fontaine, M. Numerical Analysis of the Contribution of the Transverse Asymmetry in the Photo-Induced Index Change Profile to the Birefringence of Optical Fiber. *J. Lightwave Technol.* **2002**, *20*, 1463–1470. [[CrossRef](#)]
21. Vengsarkar, A.M.; Zhong, Q.; Inniss, D.; Reed, W.A.; Kosinski, S.G. Birefringence reduction in side-written photoinduced fiber devices by a dual-exposure method. *Opt. Lett.* **1994**, *19*, 1260–1262. [[CrossRef](#)] [[PubMed](#)]
22. Lu, Y.C.; Huang, W.P.; Jian, S.S. Full Vector Complex Coupled Mode Theory for Tilted Fiber Gratings. *Opt. Express* **2010**, *18*, 713–726. [[CrossRef](#)] [[PubMed](#)]
23. Hill, K.O.; Malo, B.; Bilodeau, F.; Johnson, D.C.; Albert, J. Bragg gratings fabricated in monomode photosensitive optical fiber by UV exposure through a phase mask. *Appl. Phys. Lett.* **1993**, *62*, 1035–1037. [[CrossRef](#)]
24. Huang, J.; Zhou, Z.; Zhang, D.; Chen, J.; Deng, X. Design and Application of a Fiber Bragg Grating Tension Sensor for Anchor Rope. *Adv. Mech. Eng.* **2013**, *6*, 995–1001. [[CrossRef](#)]
25. Ma, G.M.; Li, C.R.; Quan, J.T.; Jiang, J.; Cheng, Y.C. A Fiber Bragg Grating Tension and Tilt Sensor Applied to Icing Monitoring on Overhead Transmission Lines. *IEEE Trans. Power Deliv.* **2011**, *26*, 2163–2170. [[CrossRef](#)]